Journal of Chemistry and Technologies, 2024, *32*(2), 456-464

Journal of Chemistry and Technologies

pISSN 2663-2934 (Print), ISSN 2663-2942 (Online).

journal homepage: http://chemistry.dnu.dp.ua
editorial e-mail: chem.dnu@gmail.com

UDC 542.61.547

INFLUENCE OF SYNTHESIS CONDITIONS ON THE STRUCTURAL AND MAGNETIC PROPERTIES OF $CoFe_2O_4$

Liliya A. Frolova[1*], Alexander S. Baskevich[1], Irina V. Sknar[1], Oleksandr I. Kushnerov[2]
[1]*Ukrainian State University of Chemical Technology, Dnipro, Ukraine*
[2]*Oles Honchar Dnipropetrovsk National University, Dnipro, Ukraine*
Received 1 May 2024; accepted 7 June 2024; available online 10 July 2024

Abstract

The article proposes the synthesis of $CoFe_2O_4$ by a modified coprecipitation method followed by plasma treatment. With the help of simplex planning of the experiment, the samples were synthesized using different precipitants. X-ray phase analysis and vibrational magnetometry were used to characterize the obtained samples. Diagrams of the composition of the precipitator and the response function are given in the paper. Alkalis in the NaOH - LiOH - KOH system were used as precipitants. The response functions were a coercive force, saturation magnetization, average crystallite size, crystallite size along the X-ray pattern line (311), crystallite size along the X-ray pattern line (400), dislocation density, and percentage of microstrains. Summarizing the results of mathematical modeling and graphical display of experimental data, presented in the form of composition-property diagrams, made it possible to quantitatively assess the influence of the nature of the precipitant on the structural and magnetic properties of cobalt ferrites. The saturation magnetization for samples obtained using sodium hydroxide is higher than for other samples. High saturation magnetization values also apply to samples along the NaOH-LiOH line. It is established that isolines corresponding to high values of saturation magnetization coincide with larger values of the lattice parameter. An inverse relationship is observed for the values of microstresses and the density of dislocations. That is, a more perfect crystal structure corresponds to improved magnetic properties. X-ray phase analysis also showed that the presence of impurities reduces the saturation magnetization and increases the coercive force.

Keywords: precipitation; sodium hydroxide; simplex-lattice planning of the experiment; response function.

ВПЛИВ УМОВ СИНТЕЗУ НА СТРУКТУРНІ І МАГНІТНІ ВЛАСТИВОСТІ $CoFe_2O_4$

Лілія А. Фролова[1*], Олександр С. Баскевич[1], Ірина В. Скнар[1], Олександр І. Кушнеров[2]
[1] *ДВНЗ «Український державний хіміко-технологічний університет», просп.Гагаріна, 8, Дніпро,49005, Україна*
[2]*Дніпровський національний університет імені Олеся Гончара, просп. Гагаріна, 72, Дніпро, 49010, Україна*

Анотація

У роботі запропоновано синтез $CoFe_2O_4$ модифікованим методом співосадження з наступною плазмовою обробкою. За допомогою симплекс-решітчастого планування експерименту були синтезовані зразки з використанням різноманітних осаджувачів. Для характеристики отриманих зразків було використано рентгенофазовий аналіз, вібраційну магнітометрію. В роботі представлені діаграми «склад осаджувача – функція відгука». В якості осаджувачів використовували луги в системі NaOH - LiOH – KOH. Функціями відгуку були коерцитивна сила, намагніченість насичення, середній розмір кристалітів, розмір кристалітів по лінії рентгенограми (311), розмір кристалітів по лінії рентгенограми (400), щільність дислокацій, відсоток мікронапружень. Узагальнення результатів математичного моделювання та графічного відображення експериментальних даних, що представлені в вигляді діаграм «склад – властивість», дозволили кількісно оцінити вплив природи осаджувача на структурні та магнітні властивості феритів кобальту. Намагніченість насичення для зразків, що отримані з застосуванням натрій гідроксиду, вища за інші зразки (Ms становить 136.0 А м²/кг за умови використання NaOH). Високі показники намагніченості насичення відносяться також до зразків по лінії NaOH-LiOH. Встановлено, що ізолінії, які відповідають високим значенням намагніченості насичення, співпадають з більшими значеннями параметра решітки. Зворотня залежність спостерігається для значень мікронапруг та густини дислокацій. Тобто довершеніша кристалічна структура відповідає покращеним магнітним властивостям. Також рентгенофазовий аналіз показав, що наявність домішок знижує намагніченість насичення та підвищує коерцитивну силу.

Ключові слова: осадження; натрій гідроксид; симплекс-решітчасте планування експерименту; функція відгуку.

**Corresponding author: e-mail: 19kozak83@gmail.com*

doi: 10.15421/jchemtech.v32i2.303152

Journal of Chemistry and Technologies, 2024, *32*(2), 456-464

Introduction

The rapid development of science-intensive technologies leads to the expansion of the areas of use of spinel ferrites [1–3]. At the beginning of the century, their field of use was limited to the creation of magnets and magnetic recording devices. Currently, spinel ferrites and in particular cobalt ferrites are used in environmental protection technologies (as adsorbents, photocatalysts), in medicine (as antibacterial agents and for targeted drug delivery), as sensors, in electronics, in the production of "green fuel", supercapacitors [4–9]. This is because cobalt ferrites are easily synthesized, heat-resistant, corrosion-resistant, and have high values of coercive force and saturation magnetization. Previous studies have shown that the properties of cobalt ferrite are determined by the composition, technology, and conditions of their production [10–12]. It is obvious that the complex of properties is determined by the dispersion of particles, the arrangement of cations on the octa- and tetra-sites of the ferrite crystal lattice, and the presence of non-magnetic impurities. The development of new technologies and the determination of optimal conditions for obtaining cobalt ferrite, which is most in demand on the market, are the subject of many studies [13–17].

The analysis of the results of the influence of various factors on the quality of complex oxides gives grounds for asserting that the temperature, concentration of starting substances, and pH of the starting solution are very important in the production technology of cobalt ferrite [18–20]. The influence of the nature of the precipitant is also a very important factor, but little studied. The choice of the appropriate reagent is influenced by such factors as reaction speed, buffering capacity, solubility, price and availability of the reagent, and easy and inexpensive transportation of the reagent. In the practice of producing ferrites, salts or oxides are used as precursors, depending on the technology of their production. In liquid-phase technologies, salt solutions and an alkaline precipitant are mandatory precursors.

During precipitation from solutions of metal salts, in particular iron (II), by various precipitants, such as hydroxides, carbonates, and bicarbonates of alkali metals and ammonium, various basic salts are precipitated, which has a strong influence on the structure and properties of the compounds obtained from them, for example, oxides metals [21].

The range of alkaline agents is quite wide. All of them have certain advantages and disadvantages. When using inexpensive precipitants such as sodium carbonates, calcium hydroxide, calcium oxide, slaked dolomite lime, and quick dolomite lime, the formation of high-quality cobalt ferrite is impossible due to contamination with poorly soluble calcium and magnesium sulphates.

The mechanism of precipitation from solutions of iron(II) salts by soluble carbonates and bicarbonates of alkali metals and ammonium is usually presented in a simplified manner, assuming that iron(II) carbonate is formed as a result of the reaction. However, due to the ability to hydrolyse the carbonate ion, carbonate ions, bicarbonate ions, and hydroxide ions are present in the solution. This can lead to the formation of ferric carbonate, ferric hydroxide, and ferric hydroxocarbonate. Research on the possibility of using carbonates is considered in works [22; 23].

The use of ammonia complicates the technological scheme, which requires ensuring the necessary working conditions. Homogeneous methods of precipitation of hydroxides are promising. One of them uses products of high-temperature hydrolysis of urea. This allows you to regulate the process of formation of embryos and their further growth. In addition, it is possible to use hydroxides of lithium, potassium, and sodium, which differ in the size of the cation and the degree of dissociation.

The purpose of this study is to determine the influence of the nature of the precipitant on the magnetic properties of cobalt ferrite using the simplex lattice experiment planning method.

Method

The following reagents were used in the experimental studies: $CoSO_4$, $FeSO_4\ 7H_2O$; trilon B; NaOH, LiOH, KOH.

The following conditions were adopted for the research: concentration of $FeSO_4$, $CoSO_4$ – 0.5 mol/l, concentration of precipitants – 1.0 mol/l, temperature – 40 °C.

The synthesis was carried out in a plasma reactor, the principle of which is described in detail in [17].

X-ray phase analysis was performed using a DRON-2 diffractometer.

To study the influence of the composition of precipitants on the properties of ferrites, a simplex lattice plan was used, which requires a minimum number of experiments to study the dependence of the response function on the selected factors. Molar concentrations of sodium hydroxide, lithium, and potassium, respectively, were chosen

Journal of Chemistry and Technologies, 2024, *32*(2), 456-464

as factors x_1, x_2, and x_3. The plan of the experiment is given in Table 1.

Table 1

Simplex lattice planning matrix {3,3}

№	Composition of the precipitator			
	NaOH	KOH	LiOH	Yi
1	1	0	0	y_1
2	0.667	0.333	0	y_2
3	0.333	0.667	0	y_3
4	0	1	0	y_4
5	0	0.667	0.333	y_5
6	0	0.333	0.667	y_6
7	0	0	1	y_7
8	0.333	0	0.667	y_8
9	0.667	0	0.333	y_9
10	0.333	0.333	0.333	y_{10}

Calculation of coefficients in the regression equation and verification of its adequacy was carried out using the STATISTICA 12 program. "Property-composition" diagrams were depicted using isolines. The response functions were coercive force (Hc), Oe; saturation magnetization (Ms), Emu/g; crystallite size (L, A); the size of the crystallites along the X-ray line 311 (L_{311}, A); the size of the crystallites along the X-ray line 400 (L_{400}, A); density of dislocations ($Ds_{(311)}$) sm^{-2}), percentage of microstresses (M, %).

Results and discussion

The magnetic and structural characteristics of cobalt ferrite are the most important properties. Table 2 shows the matrix of the results of the implementation of the simplex-lattice plan used to study the effect of the nature of the precipitator the values of the response functions obtained for the coded conditions adopted in each experiment and the serial number of the samples. The table also shows the phase composition of the samples determined by X-ray phase analysis.

Table 2

Results of simplex planning of the experiment

№	Hc, Oe	Ms, Emu/g	a, A	L_{311}, A	L_{400}, A	L, A	$M*10^{-3}$, %	$D_{311}*10^{10}$, sm^{-2}	Phase composition
1	300	136	8.3449	387	552	485	0.66	48.9	$CoFe_2O_4$
2	750	51.86	8.3363	349	489	438	0.67	80.2	$CoFe_2O_4$
3	450	28.34	8.3306	305	402	383	0.506	78.7	$CoFe_2O_4$. CoOOH
4	400	31.5	8.3363	414	582	519	0.573	42.7	$CoFe_2O_4$. FeOOH
5	300	18.174	8.3249	227	399	284	2.12	142	$CoFe_2O_4$. CoOOH
6	400	37.45	8.3406	256	488	320	2.39	112	$CoFe_2O_4$. CoOOH
7	750	77.275	8.3373	425	612	533	0.63	40.5	$CoFe_2O_4$. FeOOH. CoOOH
8	650	41.285	8.3458	796	612	370	2.12	83.8	$CoFe_2O_4$.CoO.CoOOH
9	800	93.25	8.3411	469	629	1170	0.96	44.1	$CoFe_2O_4$. CoOOH
10	400	36	8.3373	223	461	238	2.83	147	$CoFe_2O_4$. FeOOH. CoOOH

Figures 1–7 illustrate contour plots of the effect of the nature and ratio of precipitants on the magnetic and structural properties of cobalt ferrite. resulting from the formation of certain products due to the interaction of components. Various feedback values were obtained, which are indicated by a change in color. Red colored regions indicate higher values of the response function. It can be seen from Figure 1 that the saturation magnetization for samples obtained using sodium hydroxide is higher than in other samples (Ms is 136.0 Emu/g for sample 1 and 93.25 Emu/g for sample 9). High values of saturation magnetization also apply to samples along the NaOH-LiOH line.

Journal of Chemistry and Technologies, 2024, *32*(2), 456-464

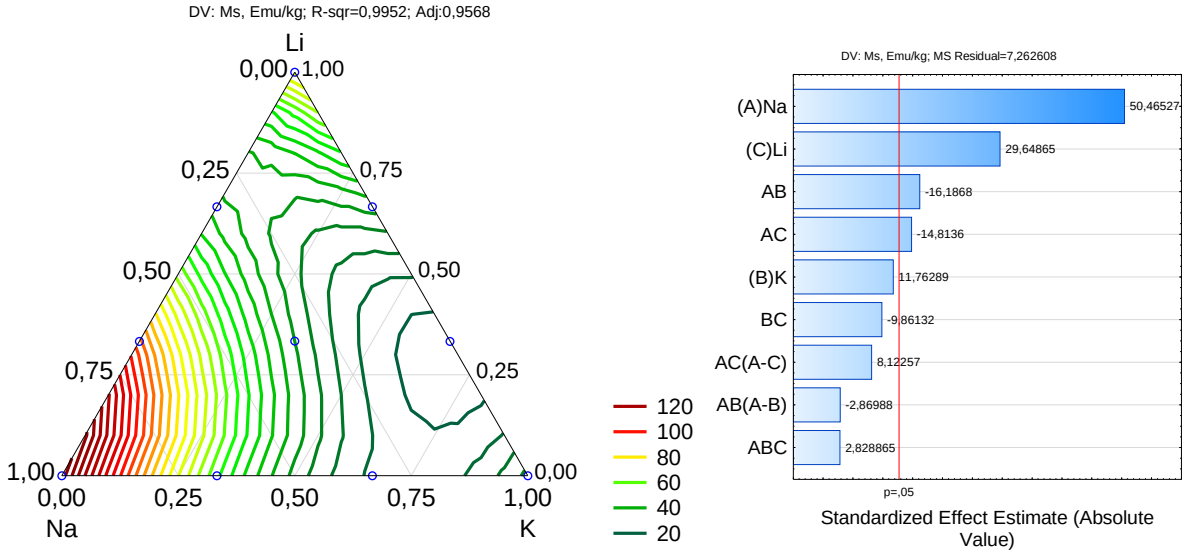

a) **b)**

$$M_s = 136.00 \cdot x_1 + 30.89 \cdot x_2 + 77.878 \cdot x_3 - 195.07 \cdot x_1 \cdot x_2 - 178.52 \cdot x_1 \cdot x_3 - 119.59 \cdot x_2 \cdot x_3 + 248.572 \cdot x_1 \cdot x_2 \cdot x_3 - 77.72 \cdot x_1 \cdot x_2 \cdot (x_1 - x_2) + 219.982 \cdot x_1 \cdot x_3 \cdot (x_1 - x_3)$$

Fig. 1. Dependence of saturation magnetization on the composition of the precipitator (a) and Pareto diagram of standardized effects (b)

Analysis of the Pareto diagram indicates that the most influential component of the precipitant is sodium hydroxide. followed by lithium hydroxide.

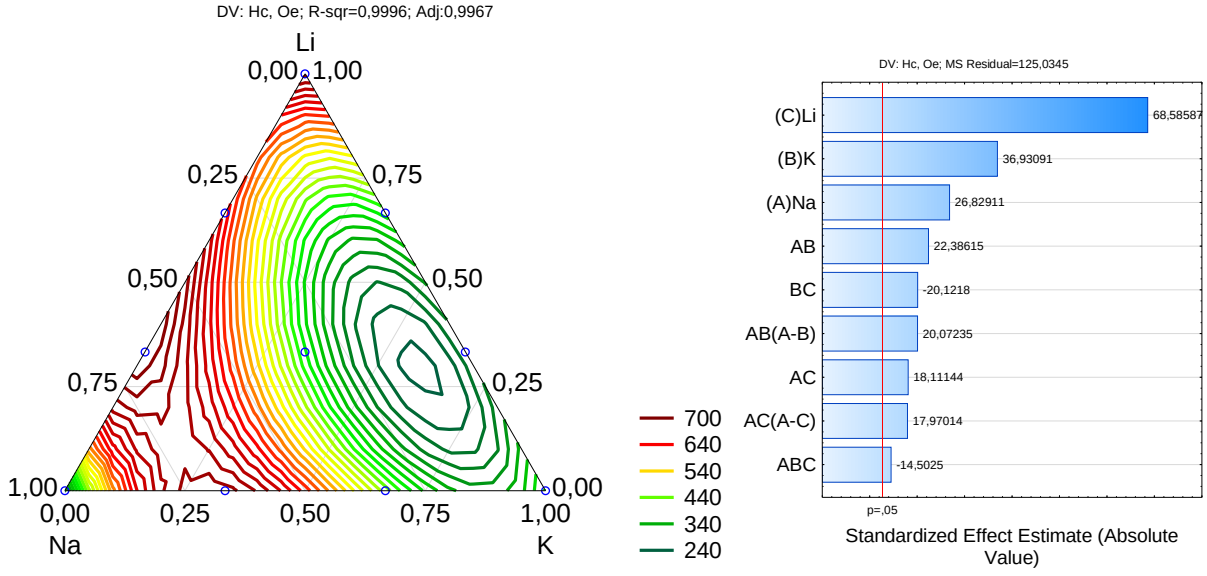

a) **b)**

$$Hc = 300.00 \cdot x_1 + 402.50 \cdot x_2 + 747.50 \cdot x_3 - 1119.38 \cdot x_1 \cdot x_2 + 905.63 \cdot x_1 \cdot x_3 - 1012.51 \cdot x_2 \cdot x_3 - 5287.51 \cdot x_1 \cdot x_2 \cdot x_3 + 2255.60 \cdot x_1 \cdot x_2 \cdot (x_1 - x_2) + 2019.36 \cdot x_1 \cdot x_3 \cdot (x_1 - x_3)$$

Fig. 2. Dependence of the coercive force on the composition of the precipitant (a) and the Pareto diagram of standardized effects (b)

Fig. 2 shows a contour plot showing the optimal value of the composition of the precipitant (NaOH-LiOH-KOH) for increasing the coercive force. This graph clearly shows that the amount of coercive force increases along the sodium hydroxide-lithium hydroxide line with a small amount of potassium hydroxide.

In addition, the correlation of the experimental data from the simplex lattice design with the predicted values using the cubic model was high. with an R^2 value > 99.99 %. indicating that the

model can adequately explain the discrepancy between the data. Moreover, the values of the correlation coefficient for the obtained models were lower than 86 % for all calculations (Fig. 1–7), which means that the linear model cannot adequately describe the magnetic properties of cobalt ferrite. Checking the models (Figs. 1–7) also showed that the cubic model adequately describes the saturation magnetization, coercive force, lattice parameter, crystallite size, dislocation density and percentage of microstresses. On the contrary, the linear model does not sufficiently take into account the influence of sodium hydroxide. This means that the linear model was missing the most important predictor variable (precipitator interaction effect), which is necessary to successfully predict the effect of mixed precipitants on the value of the magnetic properties of cobalt ferrite.

Figure 3 shows that larger lattice parameter values correspond to sodium hydroxide-lithium hydroxide compositions and coincide with regions of increased saturation magnetization values.

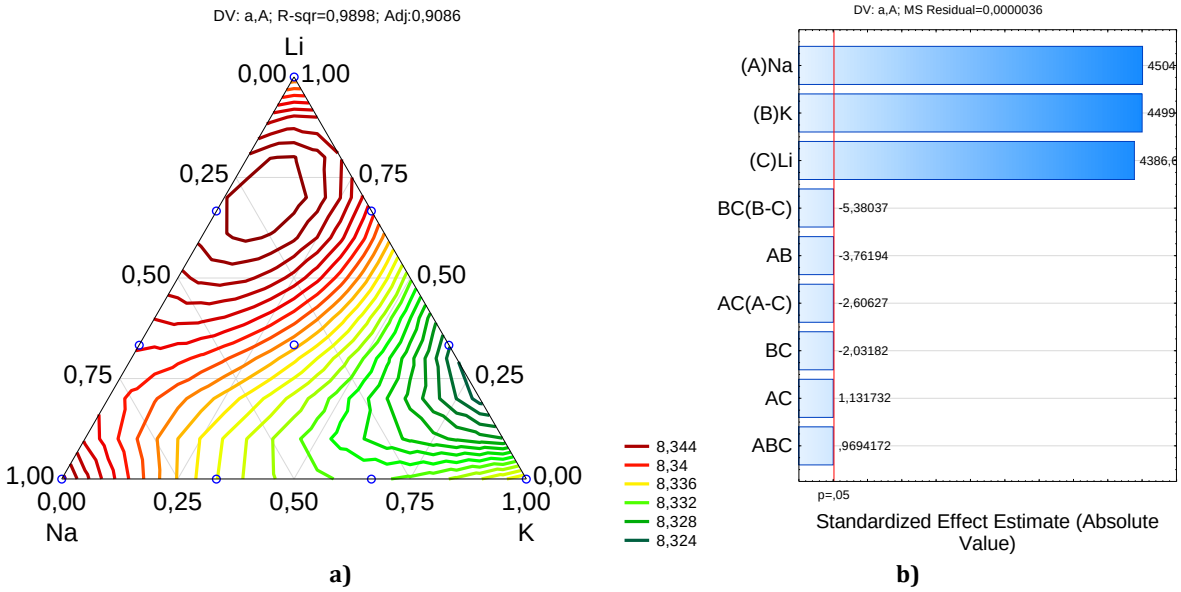

a) **b)**

$$a = 8.345325 \cdot x_1 + 8.335875 \cdot x_2 + 8.3373 \cdot x_3 - 0.0322 \cdot x_1 \cdot x_2 + 0.0096 \cdot x_1 \cdot x_3 - 0.01726 \cdot x_2 \cdot x_3 + 0.0601 \cdot x_1 \cdot x_2 \cdot x_3 - 0.049 \cdot x_1 \cdot x_2 \cdot (x_1 - x_2) - 0.1027 \cdot x_1 \cdot x_3 \cdot (x_1 - x_3)$$

Fig. 3. Dependence of the lattice parameter on the composition of the precipitator (a) and the Pareto diagram of standardized effects (b)

Crystallite size values were calculated using three methods. First, according to Scherrer's formula. which in crystallography and X-ray diffraction relates the size of the crystallites to the width of the diffraction peaks. However, in addition to peak broadening due to crystallite size. there are other factors that can contribute to peak widths in X ray patterns. As a rule, these are distortions and defects of the crystal lattice, the presence of dislocations, packing defects, microstresses, the presence of grain boundaries and subboundaries, chemical heterogeneity [24]. Scherrer's formula is suitable for determining only estimated particle sizes due to the fact that such calculations are used for crystals whose sizes are less than 100–200 nm and take into account the broadening of diffraction reflexes associated with size effects only. The Williamson-Hall method [24] is used to more accurately determine particle sizes using X ray patterns. This method is based on a combination of Scherrer and Stokes-Wilson formulas. Thus, it is possible to take into account the broadening of reflexes caused by both particle sizes and microvoltages in the crystal. Thus, the sizes of the crystallites were determined by the Williamson-Hall method based on the (311) and (400) peaks on the X-ray diffraction pattern corresponding to certain planes. The resulting dependencies are presented in Figures 4–6. For all calculated values, general trends in crystallite size change are observed. The calculated average values of crystallites range from 10–110 nm. They are 40–60 nm along the (400) plane, and 20–80 nm along the (311) plane. It is the isolines of the crystallite sizes calculated by the Selyakov-Scherrer formula that correlates with the dependence of the saturation magnetization on the composition.

Journal of Chemistry and Technologies, 2024, *32*(2), 456-464

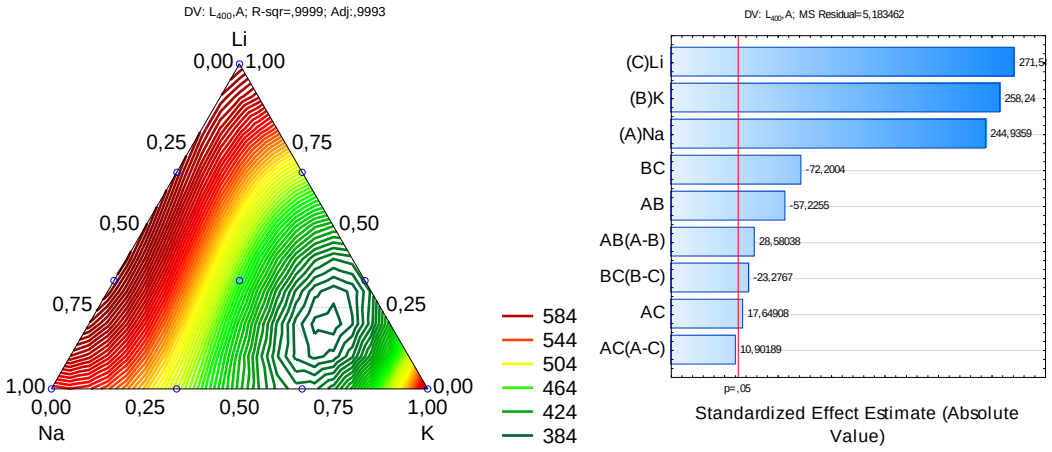

a **b**

$$L_{400} = 552.314 \cdot x_1 + 582.314 \cdot x_2 + 612.314 \cdot x_3 - 550.288 \cdot x_1 \cdot x_2 + 169.716 \cdot x_1 \cdot x_3 - 694.288 \cdot x_2 \cdot x_3 + 654.742 \cdot x_1 \cdot x_2 \cdot x_3 + 249.749 \cdot x_1 \cdot x_2 \cdot (x_1 - x_2) - 533.241 \cdot x_1 \cdot x_3 \cdot (x_1 - x_3)$$

Fig. 4. Dependence of crystallite size along line (400) on the composition of the precipitator (a) and the Pareto diagram of standardized effects (b)

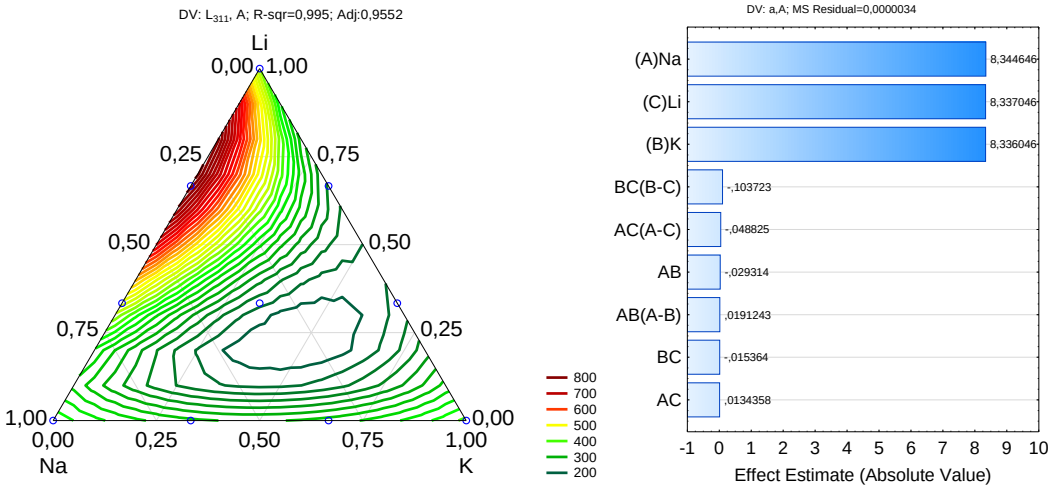

a) **b)**

$$L_{311} = 387.00 \cdot x_1 + 410.20 \cdot x_2 + 428.80 \cdot x_3 - 322.20 \cdot x_1 \cdot x_2 + 1010.70 \cdot x_1 \cdot x_3 - 801.00 \cdot x_2 \cdot x_3 - 4675.50 \cdot x_1 \cdot x_2 \cdot x_3 + 349.20 \cdot x_1 \cdot x_2 \cdot (x_1 - x_2) - 2113.17 \cdot x_1 \cdot x_3 \cdot (x_1 - x_3)$$

Fig. 5. Dependence of crystallite size along line (311) on the composition of the precipitator (a) and Pareto diagram of standardized effects (b)

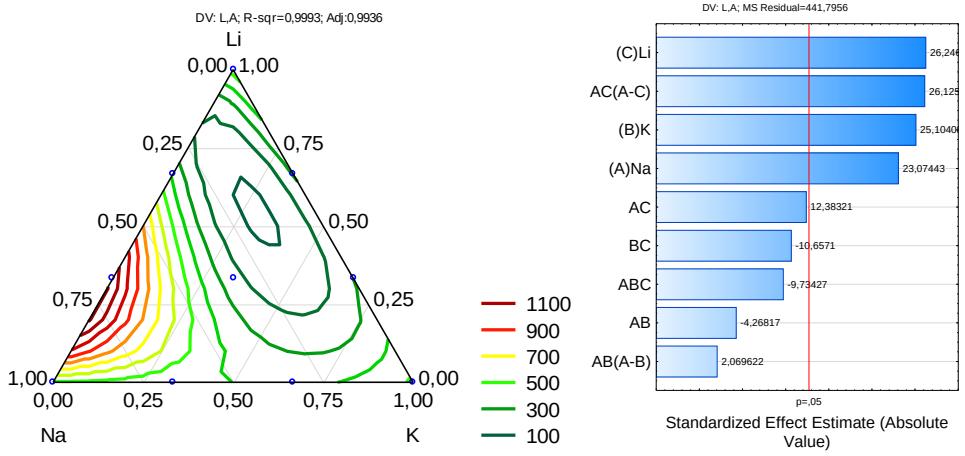

a) **b)**

$$L = 485.00 \cdot x_1 + 514.30 \cdot x_2 + 537.70 \cdot x_3 - 401.18 \cdot x_1 \cdot x_2 + 1163.93 \cdot x_1 \cdot x_3 - 1008.01 \cdot x_2 \cdot x_3 - 6671.25 \cdot x_1 \cdot x_2 \cdot x_3 + 437.17 \cdot x_1 \cdot x_2 \cdot (x_1 - x_2) + 5518.49 \cdot x_1 \cdot x_3 \cdot (x_1 - x_3)$$

Fig. 6. Dependence of the average size of crystallites on the composition of the precipitant (a) and the Pareto diagram of standardized effects (b)

Journal of Chemistry and Technologies, 2024, *32*(2), 456-464

On the contrary. high values of dislocation density and microstresses correspond to lower values of saturation magnetization and coercive force (Figs. 7, 8).

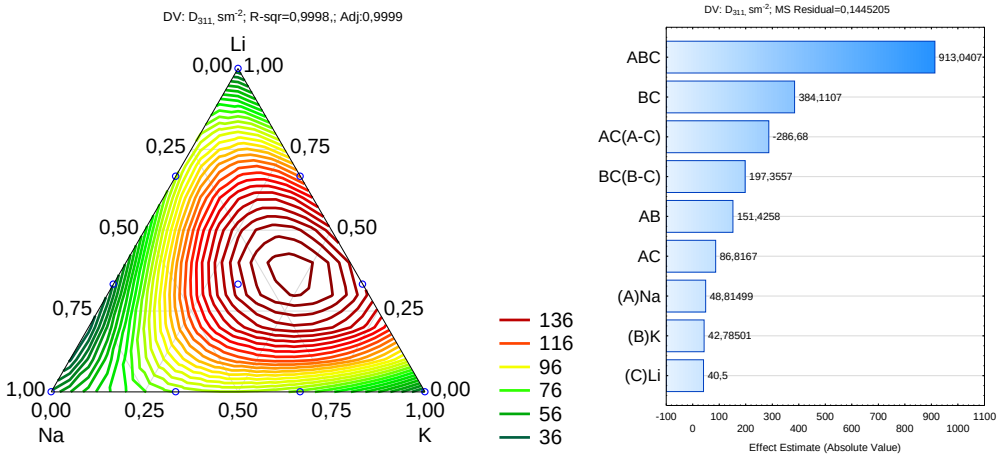

a) **b)**

$$D_{311} = 48.815 \cdot x_1 + 42.785 \cdot x_2 + 40.500 \cdot x_3 + 151.43 \cdot x_1 \cdot x_2 + 86.817 \cdot x_1 \cdot x_3 + 384.111 \cdot x_2 \cdot x_3 + 913.041 \cdot x_1 \cdot x_2 \cdot x_3 - 286.68 \cdot x_1 \cdot x_2 \cdot (x_1 - x_2) + 197.356 \cdot x_1 \cdot x_3 \cdot (x_1 - x_3)$$

Fig. 7. Dependence of the density of dislocations on the composition of the precipitant (a) and the Pareto diagram of standardized effects (b)

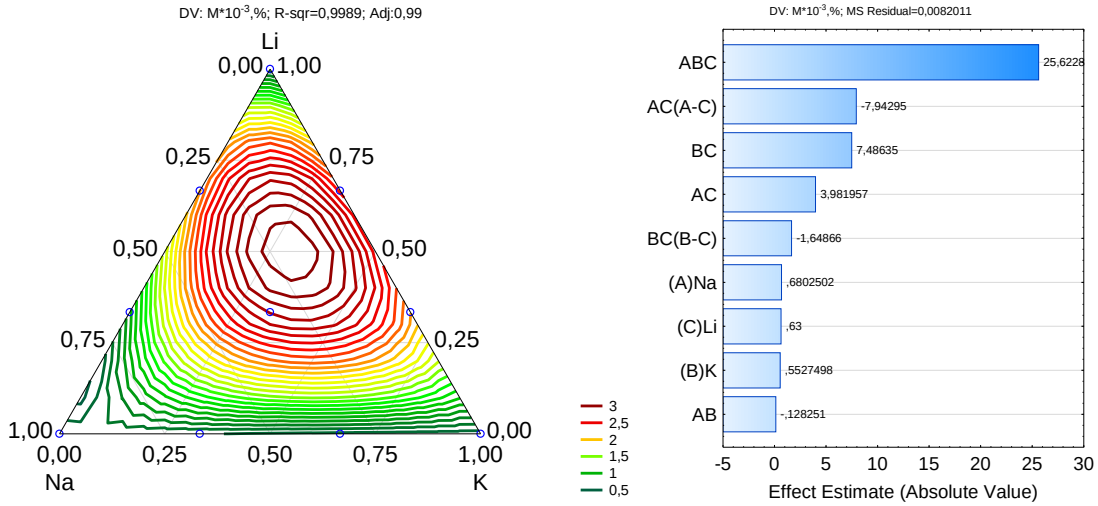

a) **b)**

$$M = 0.680 \cdot x_1 + 0.5527 \cdot x_2 + 0.630 \cdot x_3 - 0.1282 \cdot x_1 \cdot x_2 + 3.98 \cdot x_1 \cdot x_3 + 7.486 \cdot x_2 \cdot x_3 + 25.622 \cdot x_1 \cdot x_2 \cdot x_3 - 7.942 \cdot x_1 \cdot x_2 \cdot (x_1 - x_2) - 1.648 \cdot x_1 \cdot x_3 \cdot (x_1 - x_3)$$

Fig. 8. Dependence of the percentage of microstresses on the composition of the precipitator (a) and the Pareto diagram of standardized effects (b)

Conclusions

The analysis of the composition-property diagrams, which were constructed by the method of simplex-lattice planning of the experiment, made it possible to obtain new data on the influence of the nature of the precipitant on the magnetic and structural properties of cobalt ferrite. Coercive force, saturation magnetization, average crystallite size, crystallite size along the X-ray diagram line (311), crystallite size along the X-ray diagram line (400), dislocation density, and percentage of microstrains were selected as response functions.

The effect of the nature and concentration of alkali on the magnetic properties of cobalt ferrite nanoparticles at constant values of other parameters was studied. Such alkalis as sodium, potassium, and lithium hydroxides were used.

It was established that the magnetic characteristics of cobalt ferrite increase in the order: of NaOH > LiOH > KOH. The decrease in saturation magnetization when using stronger bases is due to the possibility of the formation of non-magnetic phases.

That is, a more perfect crystal structure corresponds to improved magnetic properties. X-ray phase analysis also showed that the presence of impurities reduces the saturation magnetization and increases the coercive force.

References

[1] Salih, S. J., Mahmood, W. M. (2023). Review on magnetic spinel ferrite (MFe_2O_4) nanoparticles: From synthesis to application. *Heliyon*., *9*(6), E16601. https://doi.org/10.1016/j.heliyon.2023.e16601

[2] Liandi, A. R., Cahyana, A. H., Kusumah, A. J. F., Lupitasari, A., Alfariza, D. N., Nuraini, R., Kusumasari, F. C. (2023). Recent trends of spinel ferrites (MFe_2O_4: Mn, Co, Ni, Cu, Zn) applications as an environmentally friendly catalyst in multicomponent reactions: A review. *Case Studies in Chemical and Environmental Engineering*, *7*, 100303. https://doi.org/10.1016/j.cscee.2023.100303

[3] Dastjerdi, O. D., Shokrollahi, H., Mirshekari, S. (2023). A review of synthesis, characterization, and magnetic properties of soft spinel ferrites. *Inorganic Chemistry Communications*, 110797. https://doi.org/10.1016/j.inoche.2023.110797

[4] Benlembarek, M., Salhi, N., Benrabaa, R., Djaballah, A. M., Boulahouache, A., Trari, M. (2022). Synthesis, physical and electrochemical properties of the spinel $CoFe_2O_4$: application to the photocatalytic hydrogen production. *International Journal of Hydrogen Energy*, *47*(15), 9239–9247. https://doi.org/10.1016/j.ijhydene.2021.12.270

[5] Rani, B., Nayak, A. K., Sahu, N. K. (2021). Electrochemical supercapacitor application of $CoFe_2O_4$ nanoparticles decorated over graphitic carbon nitride. *Diamond and Related Materials*, *120*, 108671. https://doi.org/10.1016/j.diamond.2021.108671

[6] Mariosi, F. R., Venturini, J., da Cas Viegas, A., Bergmann, C. P. (2020). Lanthanum-doped spinel cobalt ferrite ($CoFe_2O_4$) nanoparticles for environmental applications. *Ceramics International*, *46*(3), 2772–2779. https://doi.org/10.1016/j.ceramint.2019.09.266

[7] Abraime, B., El Maalam, K., Fkhar, L., Mahmoud, A., Boschini, F., Tamerd, M. A., Mounkachi, O. (2020). Influence of synthesis methods with low annealing temperature on the structural and magnetic properties of $CoFe_2O_4$ nanopowders for permanent magnet application. *Journal of Magnetism and Magnetic Materials*, *500*, 166416. https://doi.org/10.1016/j.jmmm.2020.166416

[8] Modabberasl, A., Pirhoushyaran, T., Esmaeili-Faraj, S. H. (2022). Synthesis of $CoFe_2O_4$ magnetic nanoparticles for application in photocatalytic removal of azithromycin from wastewater. *Scientific Reports*, *12*(1), 19171. https://doi.org/10.1038/s41598-022-21231-2

[9] Foroutan, R., Peighambardoust, S. J., Mohammadi, R., Peighambardoust, S. H., Ramavandi, B. (2022). Application of waste chalk/$CoFe_2O_4$/K_2CO_3 composite as a reclaimable catalyst for biodiesel generation from sunflower oil. *Chemosphere*, *289*, 133226. https://doi.org/10.1016/j.chemosphere.2021.133226

[10] Akhtar, S., Slimani, Y., Almessiere, M. A., Baykal, A., Polat, E. G., Caliskan, S. (2023). Influence of Tm and Tb co-substitution on structural and magnetic features of $CoFe_2O_4$ nanospinel ferrites. *Nano-Structures & Nano-Objects*, *33*, 100944. https://doi.org/10.1016/j.nanoso.2023.100944

[11] Das, A., Palliyan, A. J., Sahoo, A. K., Mohanty, J. R., Gorige, V. (2023). Structure, magnetic morphology and magnetization correlations in pulsed laser deposited $CoFe_2O_4$ (111) thin films. *Thin Solid Films*, *770*, 139763. https://doi.org/10.1016/j.tsf.2023.139763

[12] Kuekha, R., Mubarak, T. H., Azhdar, B. (2023). Synthesis, structural, magnetic, and dielectric properties of Ni^{2+}, Mn^{2+} Co-substituted $CoFe_2O_4$ nanoferrites using sol–gel auto combustion method. *Materials Science and Engineering: B*, *292*, 116411. https://doi.org/10.1016/j.mseb.2023.116411

[13] Ravindra, A. V., Ju, S. (2023). Mesoporous $CoFe_2O_4$ nanocrystals: Rapid microwave-hydrothermal synthesis and effect of synthesis temperature on properties. *Materials Chemistry and Physics*, *303*, 127818. https://doi.org/10.1016/j.matchemphys.2023.127818

[14] Prakshale, R., Bangale, S., Kamble, M., Sonawale, S. (2023). Synthesis, study and characterization of spinel $CoFe_2O_4$ for the ethanol gas-sensing applications. *Journal of Materials Science: Materials in Electronics*, *34*(27), 1852. https://doi.org/10.1007/s10854-023-11253-5

[15] Basha, B., Ikram, M., Alrowaili, Z. A., Al-Buriahi, M. S., Anwar, M., Suleman, M. (2023). Wet chemical route synthesis of Cr doped $CoFe_2O_4$@ rGO nanocomposite for photodegradation of organic effluents present in drinking water. *Ceramics International*, *49*(18), 30049–30059. https://doi.org/10.1016/j.ceramint.2023.06.262

[16] Choopannezhad, S., Hassanzadeh-Tabrizi, S. A. (2023). Synthesis of $CoFe_2O_4$-$CaCO_3$ nanocomposite for simultaneous magnetic hyperthermia and drug release applications. *Journal of Alloys and Compounds*, *960*, 170636. https://doi.org/10.1016/j.jallcom.2023.170636

[17] Frolova, L., Sukhyy, K. (2022). Investigation of the ferritization process in the Co^{2+}–Fe^{2+}–SO_4^{2-}–OH^- system under the action of contact non-equilibrium low-temperature plasma. *Applied Nanoscience*, 12, 1029–1036. https://doi.org/10.1007/s13204-021-01755-1

[18] Frolova, L., Derimova, A., Khlopytskyi, A., Galivets, Y., Savchenko, M. (2016). Investigation of phase formation in the system $Fe^{2+}/Co^{2+}/O_2/H_2O$. *Eastern-European Journal of Enterprise Technologies, 6*(6), 64–68. doi: 10.15587/1729-4061.2016.85123

[19] Frolova, L. A. (2014). Production conditions of iron oxide black from pickle liquors. *Metallurgical & Mining Industry*, (4), 65–69.

[20] Frolova, L. (2020). Photocatalytic activity of spinel ferrites $Co_xFe_{3-x}O_4$ (0.25< x< 1) obtained by treatment contact low-temperature non-equilibrium plasma liquors. *Applied Nanoscience*, *10*(12), 4585. doi:10.1007/s13204-020-01344-8

[21] Drissi, S. H., Refait, P., Abdelmoula, M., Génin, J. M. R. (1995). The preparation and thermodynamic properties of Fe (II)/ Fe (III) hydroxide-carbonate (green rust 1); Pourbaix diagram of iron in carbonate-containing aqueous media. *Corrosion science*, *37*(12), 2025-2041. https://doi.org/10.1016/0010-938X(95)00096-3

[22] Dlamini, H., Pollak, H., Coville, N. J., Van Wyk, J. A. (1999). *Influence of preparation conditions on precipitated iron oxides and hydroxides: a Moessbauer spectroscopy study* (No. IAEA-TECDOC--1069).

[23] Frolova, L. A., Derimova, A. V., Butyrina, T. E., Savchenko, M. O. (2018). An Investigation of the Mechanism Magnetite Precipitation Using Ammonium Carbonate. *Eurasian Chemico-Technological Journal*, *20*(3), 223–228. DOI: 10.18321/ectj725

[24] Himabindu, B., Devi, N. L., Kanth, B. R. (2021). Microstructural parameters from X-ray peak profile analysis by Williamson-Hall models; A review. *Materials*

Today: Proceedings, *47*, 4891–4896.
https://doi.org/10.1016/j.matpr.2021.06.256